Why the South-Pole Aitken Basin is not a Mascon. A. J. Trowbridge[1]*, B. C. Johnson[2], A. M. Freed[1], H. J. Melosh[1], and K. Graves[1], [1]Department of Earth, Atmospheric, and Planetary Sciences, Purdue University, West Lafayette, Indiana 47907, USA, [2]Department of Earth, Environmental and Planetary Sciences, Brown University, Providence, Rhode Island 02912, USA, *atrowbr@purdue.edu.

Introduction: South Pole-Aitken (SPA) basin is a large (2400 x 2050 km, [1]) elliptical basin that stretches from the south pole of the Moon to Aitken crater; it is the largest and oldest recognized impact basin on the moon. Except for SPA, all other impact basins on the Moon larger than ~200 km in diameter are mascon basins, meaning they represent a superisostatic mass even though they are regions of low topography. Mascons are identified by a positive free-air gravity anomaly (e.g. [2]). Though some mascons are the result of lithospheric support of dense mare fill, other empty (or near empty) basins show that the fill is not required. Previous combined hydrocode and finite element numerical studies have shown that mascon basins form due to uplifted mantle as a natural consequence of transient crater collapse followed by cooling and isostatic adjustment [3, 4]. What aspect of SPA's greater size or age prevented it from forming a mascon?

Recent hydrocode models [5] have constrained the impact conditions for SPA to a 170-km diameter rocky projectile, impacting at 10 km/s. However, they were unable to match current crustal thickness at the basin center, and concluded that melt pool differentiation was necessary to reproduce observations [5]. In contrast, previous studies of other lunar basins suggest that observed crust at basin centers can be explained by the flow of crust back to the basin center during transient crater collapse [3, 4]. Thus, a second important question is the origin of the crust that currently lies in the center of the SPA basin.

Here, we construct a self-consistent pair of models using a hydrocode to model impact and transient crater collapse on a short timescale (hours) and a finite element code to calculate conductive cooling and viscoelastic relaxation associated with a non-isostatic stress state over much longer timescales (10s-100s of millions of years). Our objective is to model the complete evolution of the SPA basin consistent with current observed topography (LOLA, [6]) and gravity (GRAIL, [2]) constraints. This in turn provides constraints on the impactor, and especially on initial lunar conditions at the time of impact, including the lunar thermal gradient and the thermo-mechanical properties of the lunar crust and mantle.

Modeling Approach: We used the iSALE shock physics code [7-9] for the hydrocode modeling. The runs were conducted in axisymmetric 2D with the moon treated as a spherical target with a central gravity field. The crust was modeled with the granite ANEOS equation of state (a proxy for the lunar gabbroic anorthosite crust), while the mantle and impactors were modeled with the dunite ANEOS equation of state. Our high-resolution zone contained cell sizes of 1 km and extended 1000 cells from basin center and to a depth of 500 cells.

We conducted a parameter sweep of runs varying the geothermal gradient, pre-impact crustal thickness, projectile diameter, and melt viscosity. Once the runs reached steady state, we incorporated the temperature, crustal distribution, and density structure from iSALE as the initial conditions of an axisymmetric FEM. We used the commercial code Abaqus, which capable of incorporating a temperature-dependent rheology to simulate the development of a lithosphere as the region cools. Viscoelastic flow of the crust and mantle is driven by pressure gradients associated with non-isostatic forces that arise from the basin configuration following transient crater collapse. Once the runs reached steady state, we output the topography and Moho as well as calculated the Free-air and Bouguer gravity anomalies. These outputs are then compared against elliptically averaged observations: topography (LOLA instrument), gravity (GRAIL observations), and crust mantle interface (crustal thickness maps [10]).

Results: Figure 1 illustrates our best fit run (a 170 km dunite projectile impacting a 40-km pre-impact crustal thickness with a geothermal gradient of 50 K/km at 10 km/s). Directly after impact, the associated shock wave generated a melt pool ~200 km deep and ~1000 km wide, which took ~300 Ma to cool. Initially, the crust within the inner basin is stripped and redeposited at distance from the basin center, but as the central zone oscillates around its final stable position, the crust migrates back into the basin covering the inner basin and forming a ~25 km thick crust.

After the basin reaches steady state, the topography closely matches observed values (-6 km depth; see blue line Figure 1); however, over the course of the post-isostatic adjustment (see red lines Figure 1) the inner basin is initially shallower than the observed topography. As the melt pool cools, the inner basin gradually sinks and approaches observed depths. While the overall displacement of the inner basin is an uplift of only 1 km, the Free-air gravity signature increases significantly (~300 mGal) with the final steady state result being within a standard deviation of observations; this large change in gravity is associated with the cooling and densification of the hottest region of the melt pool.

Previous hydrocode models [5] were unable to reproduce observed crustal thickness distributions for

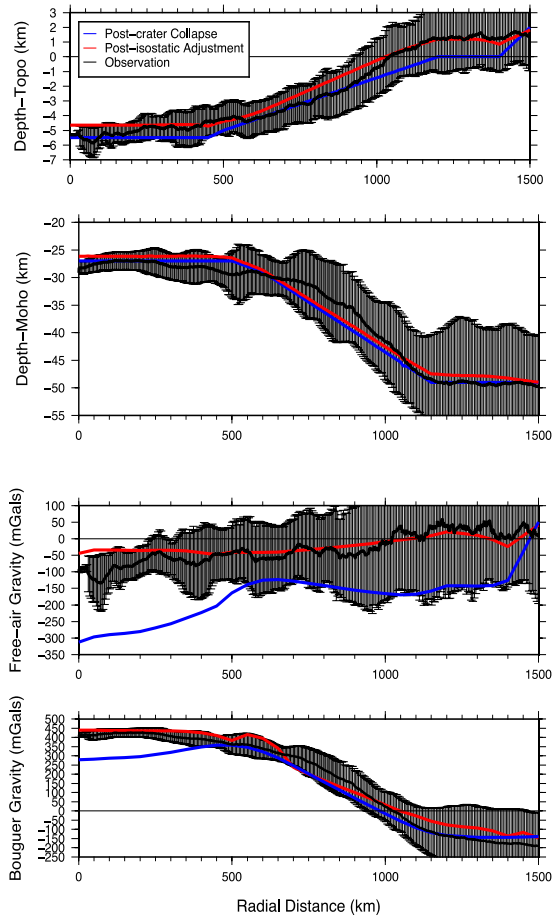

Figure 1. Comparison of post-crater collapse and post-isostatic adjustment for (top-bottom) topography, moho, Free-air gravity, and Bouguer gravity. The black error bars illustrate one standard deviation from observation. Azimuthal averages are based on an elliptical basin with axis ratios 1.35.

the basin center. They concluded that the pool of melted material produced by the SPA forming impact needed to differentiate to form the observed crust within the basin center; however, our modeling does not require this caveat to match observed crustal distributions. The crucial modeling parameter to reproduce the crustal distribution was the melt viscosity, which is a model parameter that takes into account the shear resistance contained in realistic melts [11]. By using an order of magnitude lower melt viscosity than previous hydrocode models (10^9 Pa·s), crust migrates back into the inner basin, consistent with the GRAIL inferred crustal thickness (Figure 1). Our result indicates that with a lower melt viscosity melt differentiation is not required to reproduce observed crustal distributions.

Figure 2 illustrates the difference between the uplift of the inner basin between SPA and Freundlich-Sharonov, a 320-km-diameter mascon basin. In the simulations of the evolution of these smaller basins, uplift of the inner basin continues till 200 Ma after impact. The formation of a strong lithosphere enables the uplift of the crustal collar to contribute to the uplift of the inner basin resulting in an inner basin that is superisostatic [3, 4]. Although contractional cooling continues, the strong lithosphere keeps the inner basin superisostatic. For SPA, a sufficiently strong lithosphere never forms and contractional forces associated with the thermal cooling pull the inner basin into isostatic equilibrium. In the case of SPA, the failure to form a strong lithosphere is due to a combination of the size of SPA as well as the high geothermal gradient during impact (i.e. thin lithosphere).

Conclusions: Our best fit run for SPA matches one standard deviation of observed gravity, topography, and crustal thickness distribution without the necessity of melt differentiation. Furthermore, our results indicate that the pre-impact geotherm was much hotter for SPA than younger basins; this impairs the formation of a strong lithosphere. Eventually, the cooling of the thermal anomaly pulls the inner basin into near-isostatic equilibrium, i.e. SPA does not become a mascon.

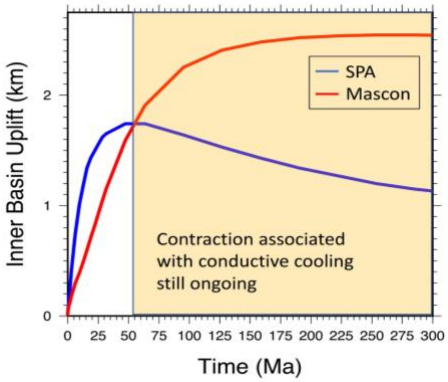

Figure 2. Comparison of uplift of the inner basis of SPA (blue) and a mascon (Freundlich-Sharonov; red).

References: [1] Garrick-Bethell, I., & Zuber, M. T. (2009) *Icarus*, **204**, 399-408. [2] Zuber, M. T., et al. (2013) *Science*, **339**, 668–671. [3] Melosh, H. J., et al. (2013) *Science*, **340**, 1552-1555. [4] Freed, A. M., et al. (2014) *J. Geophys. Res. Planets*, **119**. [5] Potter, R. W. K., et al. (2012) *Icarus*, **220**, 730–743. [6] Smith, D. E., et al. (2010) *Geophys. Res. Lett*,. **37**, L18204. [7] Amsden, A., et al. (1980) *Los Alamos National Laboratories Report*, LA-8095:101p. Los Alamos, New Mexico: LANL. [8] Collins, G. S., et al. (2004) *Meteoritics and Planetary Science*, **39**, 217-231. [9] Wünnemann, K., et al. (2006) *Icarus*, **180**, 514-27. [10] Wieczorek, M. A., et al. (2013) *Science*, **339**, 671–675. [11] Potter, R. W. K. (2012), Ph. D. Thesis, Imperial College London, London, England.

Acknowledgements: We gratefully acknowledge the developers of iSALE-2D, including Gareth Collins, Kai Wünnemann, Dirk Elbeshausen, Boris Ivanov and Jay Melosh.